

**Some Structural Observations of Self-assembling,
Fibrillar Gels Composed of Two-directional Bolaform
Arborols**

Submitted to ABSTRACTS OF THE AMERICAN CHEMICAL SOCIETY

SSRL, Stanford Linear Accelerator Center, Stanford University, Stanford, CA 94309

Work supported by Department of Energy contract DE-AC03-76SF00515.

Some Structural Observations of Self-assembling, Fibrillar Gels Composed of Two-directional Bolaform Arborols

*Jirun Sun, [#]Keunok Yu, Paul S. Russo, [&]John Pople, Alyssa Henry, Bethany Lyles,
Robin S. McCarley, [^]Gregory Baker and [^]George R. Newkome*

Department of Chemistry and Macromolecular Studies Group, Louisiana State
University, Baton Rouge, LA, 70803

[#]Department of Chemistry, Kunsan National University, Kunsan City 573-360
South Korea

[&]Stanford Synchrotron Radiation Laboratory, Menlo Park, CA 94025

[^]Department of Chemistry, University of Akron, Akron, OH 44325

Author to whom communications should be sent: Paul S. Russo (chruss@LSU.edu)

Keywords: arborol, gels, X-ray scattering, fibers, hydrogels, atomic force
microscopy, fluorescence microscopy, self assembly

Abstract

Arborols are dumbbell shaped molecules (bolaform amphiphiles) in which a hydrophobic spacer separates two hydrophilic end groups. They are a valuable model for naturally occurring fibers, such as actin or amyloid. Applications to materials science can be envisioned. On cooling from warm aqueous or methanolic solutions, arborols spontaneously assemble into long fibers. When the solutions are above a certain concentration that depends on the hydrophilic/hydrophobic balance, this leads to thermally reversible gels stabilized by a mechanism that is poorly understood. With the help of wide angle X-ray scattering, details of the arborol fiber and gel structure were obtained on wet gels. The characteristic dimensions of the fibers vary in a sensible fashion with the molecular specifics. Solvent character appears to affect the average domain length of arborols stacked into fibers. Fluorescently labeled arborols were prepared. The label does not prevent incorporation into the fibrillar structure, rendering fibril bundles visible in wet gels. Bundles are visible in concentrated gels, but not in less concentrated sols. These results are consistent with observations of dried arborols using atomic force microscopy and with previously published freeze-fracture electron microscopy and small angle X-ray scattering experiments on dried gels.

Introduction

Hydrogels are key ingredients in a number of biological systems, such as the vitreous humor of the eye and the synovial fluid that lubricates skeletal joints. They are also applied increasingly in industry—e.g., in foods, deodorants, cosmetics, and chromatography.¹ The preparation and properties of hydrogels have become active areas of investigation, consistent with their various applications.²

Several systems have been found in which the hydrogels formed by self assembly of small molecules.³⁻⁸ Arborols are small molecules that can lead to hydrogels by formation of extended fibers, similar to organogelators like the bis-urea derivatives.⁹ The factors that turn a mesh of long fibers into a true gel are not fully understood. First synthesized by Newkome *et al.*,¹⁰ arborols dissolve in warm water or water/alcohol mixtures and gel on cooling.^{11;12} The two-directional $[m]-n-[m]$ arborols consist of two hydrophilic regions, each with m terminal hydroxyl groups, connected by a linear alkyl chain with the formula C_nH_{2n} . An example appears in **Figure 1**.

The extended, fibrillar nature of arborols is reminiscent of several biological systems that form networks of extended fibers from proteins, such as F-actin¹³ and fibrinogen.¹⁴ Arborols are even more efficient in the sense that the starting molecule has a molar mass of only ~1,000 daltons. A closer biological comparison may be β -amyloid, the 4kD peptide comprising most of the plaques found in the brains of patients afflicted with Alzheimer's disease.¹⁵ When cleaved from the stable amyloid precursor protein, the β -amyloid peptide fragment assembles, in patients with insufficient capacity to clear the fragment, into the fibrous mats that characterize Alzheimer's disease. Methods for studying β -amyloid and other fibrous biogels can be developed at lower cost through arborol studies. One may also envision materials science applications of the arborols, such as stationary phases in certain separation experiments or easily removed templates around which various water-soluble monomers could be polymerized to produce highly porous materials. Arborols also provide a simple, synthetic system whose viscoelastic properties could be controlled by using temperature to adjust fiber length. Arborols provide a convenient platform for the exploration of fibrillar self-assembly and possibly the opportunity to make controlled rigid rod systems. For example, designed inhibitors could limit the rod growth to create a self-assembled system that spontaneously forms a lyotropic liquid crystalline phase, with associated optical and viscoelastic properties, that would last only so long as it's not heated. Such a system would combine the speed of small molecule liquid crystals with the material efficiency of comparatively dilute polymer lyotropic liquid crystals.

The study of arborols is still at its beginning. Fibers, or perhaps bundles of fibers, were first visualized at low resolution by fluorescence microscopy, taking advantage of a dye that fluoresces only in a hydrophobic environment such as the fiber core.¹⁶ Freeze-fracture transmission electron microscopy confirmed the presence of fibers with lengths on the micrometer scale.¹¹ Long associations of the fibers were evident, suggesting fibrils, but jamming of the fibers during the freeze step is a worrisome artifact in freeze fracture microscopy. Small angle X-ray scattering (SAXS) on dried gels supported the existence of bundled fibrillar structures.¹¹ The model shown in **Figure 2** was used to interpret the SAXS results on dried gels. The dumbbell structure of the arborols is modeled as two spheres, radius r , attached at their center by a line, length b . To simulate

fibers, the dumbbells are stacked orthogonally with a separation, a . When modeling the dried gels, the distance, a , between neighboring alkane chains was found to be ≈ 0.5 nm. The distance, b , between two hydrophilic parts of one arborols was typically 1.4 nm for most of the dried arborol gels. By modeling multiple fibers, it was found that certain features of the SAXS pattern on dried gels were consistent with multiple fibrils. It was not clear whether multiple fibrils, or bundles, were present in wet gels. Engelhardt, *et al.* studied the assembly and gelation of a dilute [9]-10-[9] solution by static and dynamic light scattering.¹⁷ The broad light scattering transitions, compared to the sharper DSC transitions, suggested that weak interconnections between fiber bundles might account for gelation. Here, we report investigations of wet gels using wide angle X-ray scattering (WAXS), atomic force microscopy (AFM) in contact mode, polarized optical microscopy (POM) and fluorescence microscopy after covalent attachment of a dye label. The results are discussed with a view towards establishing whether or not molecular specifics, such as spacer length or number of hydrophilic groups, are reflected in the wet gels, what variations may occur as a result of solvent character, and whether gel-stabilizing bundles exist in the wet gels.

Experimental

Molecular Characterization: Arborol purity was tested by proton and ^{13}C NMR, IR and MALDI-TOF mass spectrometry. In most cases, the NMR and FTIR signals met expectations.¹⁰ In FTIR, one newer preparation of [9]-12-[9] showed a small peak at 1735 cm^{-1} which suggests the existence of ester and incomplete amidization in the last step of synthesis. However, the ^{13}C and proton NMR spectra of this sample match expectations for the pure material. Ironically, this is the only arborol sample that gives an interpretable MALDI-TOF spectrum. Its observed mass (1009) is close to that of pure [9]-12-[9] (1080) less the difference between one tris(hydroxymethyl)aminomethane group (120) and the ethoxy group (45) it was supposed to displace: $1080 - 120 + 45 = 1005$. HPLC was carried out according to the same methods described in reference¹² and the results indicated that the purity of this sample was 93%. The newer [9]-12-[9] forms a gel and behaves normally in all regards.

Solution preparation. All arborols were dried in a vacuum oven at 40 °C overnight before use. All the solutions were prepared by dissolving arborols in dust-free, de-ionized water from a Barnstead Nanopure water purification system at about 80 °C.

WAXS: Wide angle X-ray scattering was carried out at Stanford Synchrotron Radiation Laboratory on beamline I-4. The distance between detector and sample was 700 mm, and the diameter of the beam stop was 6 mm. At the selected wavelength of 1.488 Å, the range of scattering vector magnitudes was from 0.48 nm⁻¹ to 15.9 nm⁻¹. The arborols were dissolved in water at about 80 °C and then loaded into X-ray capillary cells (Charles Supper) of diameter 1.0, 1.5 or 2.0 mm, centrifuged to the bottom and sealed by flame. Seven samples were prepared with five arborols ([6]-7-[6], [6]-8-[6], [6]-10-[6], [6]-11-[6] and [6]-13-[6]). The arborols were dissolved in Nanopure water or a mixture of methanol and water (volume ratio = 1:1) respectively to make a 5% solution. The samples prepared from arborols [6]-7-[6] and [6]-8-[6] did not form gel and the solubility of [6]-13-[6] in water was not high enough to make a 5% solution. A Mettler FP80 microscopy oven provided convenient and rapid temperature control. The background scattering was measured from Nanopure water at 25 °C.

Microscopy: Polarized light microscopy studies were made on an Olympus-BH outfitted with a Kodak DC290 digital camera. The [9]-12-[9] arborol was dissolved in water at about 80 °C. One end of a rectangular microslide (0.1 x 4.0 mm, Vitro Com Inc.) was flame sealed. Inserting the open end into molten [9]-12-[9] arborol solution drew it into the microslide as trapped air contracted on cooling. The solution was centrifuged to the sealed end of the microslide before gelation could take place. To evenly distribute the gel, the sealed microslides were heated again and then centrifuged.

Fluorescence Microscopy and Labeling of Arborol: The experiments were carried out on a Leitz Metallux 3 epi-illumination microscope fitted with a K2BIO confocal adapter, a Nipkow disk design.¹⁸ Images were acquired with a Dage 66 SIT (silicon-intensified target) camera. An FITC filter cube was selected. Arborols were labeled by 5-(4, 6-dichlorotriazinyl)-aminofluorescein (5-DTAF) which is an effective dye for labeling hydroxyl groups.¹⁹⁻²¹ Arborol [9]-12-[9] (0.024 mmol, 25.6 mg) was dissolved in Nanopure water to a concentration of 3 mg/ml, heated to dissolve the mixture, cooled and allowed to set for about 20 minutes until the gelation was complete. Dye (0.049 mmol 5-DTAF, 24.3 mg) was dissolved in a pH=10 sodium hydroxide solution. The solution was

poured on the top of the arborol gel and allowed to set for about 2 hours. Two layers were formed. The upper one contained unreacted 5-DTAF, and the bottom layer contained fluorescently labeled arborol gel. The upper layer was withdrawn by a pipet. The gel was first washed with pH=10 NaOH solution, and then followed by several portions of Nanopure water. The gel was dried by blowing dry nitrogen overnight. The success of labeling was confirmed by MALDI (although the values of Arborol and labeled Arborol were not correct, the difference was, as discussed in Results and Discussion). No more than 11% of the hydroxyl groups can be labeled by this procedure; the actual labeling is less as indicated by the unreacted dye.

Preparing samples for the Fluorescence Microscope: Unlabeled [9]-12-[9] arborol (25 mg) and its dyed counterpart (5 mg) were placed in a vial and dissolved in Nanopure water to a concentration of 3 mg/ml. The mixture was heated to dissolve the arborols, then cooled at room temperature to produce a strong gel. The gel was put on a cavitated microscope slide and covered by a glass cover slip, observed under the fluorescence microscope when it was wet and checked again after several hours when it was dry.

AFM: The atomic force microscope experiments were carried out on a Digital Instruments Nanoscope III multimode SPM in contact mode. The tip is a silicon nitride probe from Digital Instruments, type NP-S. The solution was applied on a freshly cleaved mica surface five minutes before putting in the microscope. Four concentrations of [9]-12-[9], 2%, 0.2%, 0.1% and 0.05% were tried. A 2% [9]-12-[9] solution was prepared by dissolving solid [9]-12-[9] in Nanopure water; 0.2% [9]-12-[9] solution was made by diluting 2% [9]-12-[9] solution in Nanopure water; 0.1% and 0.05% solutions were made by diluting 0.2% solution.

MALDI: MALDI-MS was carried out on a Bruker ProFLEX III MALDI-TOF mass spectrometer. A small amount of arborol was placed in a sample cell and covered with 200 μ L of 50% water/ethanol. The cell was suspended in a water bath and heated until the arborol dissolved. The sample was mixed with an α -cyano-4-hydroxycinnamic acid (CCA) matrix using 30% methyl cyanide (MeCN), 70% water, and 0.1% trifluoroacetic acid (TFA) as an ionizing agent.

FTIR: Samples were prepared by placing a small amount of the arborols in a mortar with slightly wet potassium bromide (KBr). The contents were ground into a fine powder and set in a die to form a translucent pellet.

Results and Discussion

Figure 3 shows that the WAXS patterns are nominally symmetrical, which indicates that there is no preferential alignment of the fibrillar structures. The effect of varying the length of the hydrophobic spacer was studied using [6]-7-[6], [6]-10-[6] and [6]-11-[6] arborols in water (**Figure 4**) and [6]-8-[6], [6]-10-[6], [6]-11-[6] and [6]-13-[6] arborols in 5% methanol/water mixtures (

Figure 5). Results are grouped in **Table 1**. A frequent observation is a peak just beyond the beamstop, at about 2.45 nm^{-1} . This feature recalls the peaks seen in *dried* fibrils at about 3 nm^{-1} in our earlier study, which were identified as side-by-side alignment of fibrils, although twist along the fibril axis cannot yet be excluded. If the peaks do represent side-by-side alignment, it is sensible for them to have shifted towards lower scattering angles in the hydrated fibrils. Other aspects of the WAXS patterns also make good sense, although they are near the limits of resolution of the experiment. The [6]-11-[6] arborol has a longer spacer chain than [6]-10-[6] and the measured b value is about 0.09 nm bigger for the former molecule. Arborol [6]-8-[6], which has the shortest spacer chain, is observed to have the largest a value (step length along the fibril). Conversely, arborol [6]-13-[6], which has the longest spacer chain, exhibits the smallest a value, but it shares that characteristic with arborol [6]-11-[6]. This suggests that a longer spacer chain permits closer approach of the molecules, but the effect tops out at eleven methylene groups. Arborol [6]-7-[6] does not form a gel at 5% in water. Its WAXS plot does not have the characteristic peak around 0.5 nm, which suggests that the dumbbells are no longer stacked orthogonally; however, the existence of peak at 1.47 nm indicates that there are some ordered arrangements.

The effects of solvent on the [6]-10-[6] and [6]-11-[6] arborols were studied. Water and a mixture of methanol and water (1:1, volume ratio) were used as solvents separately. The WAXS spacings of [6]-10-[6] and [6]-11-[6] are indicated directly in **Figure 6** and

Figure 7 respectively. The spacings are similar in both solvents, but the peak indicating distance along the fibril (parameter a) is broadened by addition of methanol, which suggests a reduction in the coherent length of the arborol stacks comprising the fibrils.

Centrifuging the sample after melting the gel led to an uneven distribution of arborols in the slice (**Figure 8A**). Under crossed polarizers in an optical microscope, the arborol gel appears to be a collection of fibers aligned at 45 or 135 degrees of angle (**Figure 8B**). The intensity of light changes periodically as the sample is rotated on the stage. Without the polarizers, the fibers appear to be randomly distributed. These observations indicate that the fibers possess birefringence, but polarized light microscopy does not clearly elucidate the structure.

Fluorescence microscopy usually provides an unambiguous contrast mechanism: one sees the labeled object (at the risk of altering the structure by the presence of the dye). The possible reaction mechanism for DTAF labeling of arborols as described in Experimental involves nucleophilic aromatic substitution by an addition-elimination pathway.²⁰ Since the selected two-directional arborol has nine hydroxyl groups at each end, it should be easy to dye, and the MALDI results confirmed this suggestion. The MALDI spectrum contains peaks around 1470 which is in the range of molecular weight for one 5-DTAF labeled [9]-12-[9]. As discussed in Experimental, the molecular weight of [9]-12-[9] we used is 1009 by MALDI and the molecular weight of 5-DTAF is 495. If one 5-DTAF is attached to a hydroxyl group, HCl will be released. So the molecular weight of labeled [9]-12-[9] is 1468, very close to the observed 1470. While this is encouraging, other species are surely present—some with no dyes attached and perhaps others with more than one dye attached. Another potential problem is that the DTAF label is not much smaller than the arborol molecule itself. To assess the behavior of the (partially) dyed arborols, the DSC melting point of a 3 wt% [9]-12-[9] unlabeled gel was compared to a 3% sample containing 2.7% unlabeled arborols and 0.3 wt% from the labeled preparation. There was no difference in the melting point with or without label. Detailed studies of the enthalpies of melting as a function of labeled content may prove revealing, but fluorescence microscopy confirms that the labeled arborols do participate in fibril formation.

When the gel was wet, the fluorescence contrast of the network to its surroundings was weak, but the fibrous textures did emit strongly enough to be caught by confocal

microscopy. **Figure 10A** is the result of a calculation by Image J software (National Institutes of Health) of three pictures, each of these an average of 50 video frames from the same spot in the microscope. Two well-focused pictures in which fibers were barely visible were summed. From this result was subtracted another picture taken slightly out of focus to reveal the structures shown in **Figure 10A**. The contrast improved after the solvent was evaporated (**Figure 10 B and C**). These figures suggest that very long fibers exist, confirming the impressions from freeze-fracture electron microscopy. The gel is not destroyed after the arborol is labeled, but it is not clear yet whether it is affected in more subtle ways that might be revealed by additional SAXS, DSC and AFM studies. If not, fluorescent labeling provides an opportunity to study the network of the gel in its native, wet state.

The atomic force microscope (AFM) can be used to check the topographical, elastic, and frictional properties of hydrogels.²²⁻²⁴ Four concentrations of [9]-12-[9], 2%, 0.2%, 0.1% and 0.05% were tried. The AFM images, **Figure 11**, were obtained in contact mode in air at room temperature. Solutions, 0.1% and 0.05% [9]-12-[9], did not produce clear AFM images. For 0.2% [9]-12-[9], the sample is not a gel. One can still see fibers, but not large bundles, in the upper part of **Figure 11**. The appearance calls to mind a network, but the fibers probably just collapsed as the solution dried to produce that illusion. A 2% [9]-12-[9] preparation does form a gel on cooling, and one can see large fiber bundles in the lower part of **Figure 11**. This is strong evidence that the bundles strengthen the gel, as suggested from the SAXS data on dried gels.²⁵ The freeze fracture EM images, with the usual risks of artifact, also suggest that the strengthening occurs as fiber bundles share individual fibers to make effective crosslinks.

Conclusion

This is the first time that WAXS has been used to check the properties of wet arborol gels. The structures found by previous studies of dried samples seem to exist in the wet gels. SAXS studies on wet gels may reveal additional parameters of the fibrils, such as thickness and how it changes during melting, addition of fiber inhibitors, etc. For arborols with 6 hydroxy groups at each end, the hydrophobic chain must include more than ten methylene groups to induce gelation.¹² If the chain length is shorter, the arborol fails to form large bundles of fibers, which are the key to form a strong gel. AFM gives

visual information on the function of bundles. At high concentration (2%) for [9]-12-[9], there are plenty of large bundles to support a gel. At low concentration (0.2%) mostly thin fibers are observed and the system does not gel. Bundles effectively crosslink the long fibers. POM confirms the birefringence of arborol gels, but the textures of the samples are not yet fully interpretable. Fluorescence microscopy on both dry and wet samples confirms the rod like structure. Covalent attachment of DTAF dye seems not to prevent incorporation of arborols into fibrillar structures.

Some questions remain. It is not understood how the fibers respond to forces such as shaking, shearing, or sonication. It is not known if a broken gel will heal through slow rearrangements of freely diffusing arborol molecules or small protofibrils. Molecules that inhibit the fibril formation could lead to control over the length, beyond thermal control, resulting in a self-assembling lyotropic liquid crystalline system or solutions with tunable viscosity. Such inhibitors can be imagined to take the form of half an arborol, and they may have unusual surface behavior. Finally, rheological and microrheological assessment of these fibrillar networks is long overdue.

Acknowledgement: We acknowledge the support of the National Science Foundation through award DMR-0075810. [XXXIfTheyChooseNotToBeAuthors:We thank Dr. Robin McCarley, Jed Aucoin and Jowell Bolivar for help with AFM.](#) JS thanks Professor George Newkome and his group for hospitality during a visit to the University of Akron.

Reference List

- (1) Abdallah, D. J.; Weiss, R. G. *Langmuir* **2000**, *16*, 352-355.
- (2) Molyneux, P. *Chemistry and Technology of Water-Soluble Polymers*; Plenum: New York, 1983; pp 1-20.
- (3) Bhattacharya, S.; Acharya, S. N. G. *Chemistry of Materials* **1999**, *11*, 3121-3132.
- (4) Franceschi, S.; de Viguerie, N.; Riviere, M.; Lattes, A. *New Journal of Chemistry* **1999**, *23*, 447-452.
- (5) Jokic, M.; Makarevic, J.; Zinic, M. *Journal of the Chemical Society-Chemical Communications* **1995**, 1723-1724.
- (6) Kogiso, M.; Ohnishi, S.; Yase, K.; Masuda, M.; Shimizu, T. *Langmuir* **1998**, *14*, 4978-4986.
- (7) Kogiso, M.; Hanada, T.; Yase, K.; Shimizu, T. *Chemical Communications* **1998**, 1791-1792.

- (8) Oda, R.; Huc, I.; Candau, S. J. *Angewandte Chemie-International Edition* **1998**, *37*, 2689-2691.
- (9) Estroff, L. A.; Hamilton, A. D. *Angewandte Chemie-International Edition* **2000**, *39*, 3447-+.
- (10) Newkome, G. R.; Baker, G. R.; Saunders, M. J.; Russo, P. S.; Gupta, V. K.; Yao, Z. Q.; Miller, J. E.; Bouillion, K. *Journal of the Chemical Society-Chemical Communications* **1986**, 752-753.
- (11) Yu, K. H.; Russo, P. S.; Younger, L.; Henk, W. G.; Hua, D. W.; Newkome, G. R.; Baker, G. *Journal of Polymer Science Part B-Polymer Physics* **1997**, *35*, 2787-2793.
- (12) Newkome, G. R.; Baker, G. R.; Saunders, M. J.; Russo, P. S.; Gupta, V. K.; Yao, Z. Q.; Miller, J. E.; Bouillion, K. *Journal of the Chemical Society-Chemical Communications* **1986**, 752-753.
- (13) Wong, G. C. L.; Tang, J. X.; Lin, A.; Li, Y. L.; Janmey, P. A.; Safinya, C. R. *Science* **2000**, *288*, 2035-+.
- (14) Madrazo, J.; Brown, J. H.; Litvinovich, S.; Dominguez, R.; Yakovlev, S.; Medved, L.; Cohen, C. *Proceedings of the National Academy of Sciences of the United States of America* **2001**, *98*, 11967-11972.
- (15) Benzinger, T. L. S.; Gregory, D. M.; Burkoth, T. S.; Miller-Auer, H.; Lynn, D. G.; Botto, R. E.; Meredith, S. C. *Biochemistry* **2000**, *39*, 3491-3499.
- (16) Newkome, G. R.; Baker, G. R.; Arai, S.; Saunders, M. J.; Russo, P. S.; Theriot, K. J.; Moorefield, C. N.; Rogers, L. E.; Miller, J. E.; Lieux, T. R.; Murray, M. E.; Phillips, B.; Pascal, L. *Journal of the American Chemical Society* **1990**, *112*, 8458-8465.
- (17) Engelhardt, T. P.; Belkoura, L.; Woermann, D. *Berichte der Bunsen-Gesellschaft-Physical Chemistry Chemical Physics* **1996**, *100*, 1064-1072.
- (18) Yin, S.; Lu, G.; Zhang, J.; Yu, F. T. S.; Mait, J. N. *Applied Optics* **1995**, *34*, 5695-5698.
- (19) Helbert, W.; Chanzy, H.; Husum, T. L.; Schulein, M.; Ernst, S. *Biomacromolecules* **2003**, *4*, 481-487.
- (20) Ahmed, F.; Alexandridis, P.; Neelamegham, S. *Langmuir* **2001**, *17*, 537-546.
- (21) Benzinger, T. L. S.; Gregory, D. M.; Burkoth, T. S.; Miller-Auer, H.; Lynn, D. G.; Botto, R. E.; Meredith, S. C. *Biochemistry* **2000**, *39*, 3491-3499.
- (22) Matzelle, T. R.; Geuskens, G.; Kruse, N. *Macromolecules* **2003**, *36*, 2926-2931.
- (23) Kurokawa, T.; Gong, J. P.; Osada, Y. *Macromolecules* **2002**, *35*, 8161-8166.
- (24) Nakayama, Y.; Nakamata, K.; Hirano, Y.; Goto, K.; Matsuda, T. *Langmuir* **1998**, *14*, 3909-3915.
- (25) Yu, K. H.; Russo, P. S.; Younger, L.; Henk, W. G.; Hua, D. W.; Newkome, G. R.; Baker, G. *Journal of Polymer Science Part B-Polymer Physics* **1997**, *35*, 2787-2793.

Table 1 Summary of WAXS results

Sample Number	1	2	3	4	5	6	7
Arborol	[6]-7-[6]	[6]-8-[6]	[6]-10-[6]	[6]-10-[6]	[6]-11-[6]	[6]-11-[6]	[6]-13-[6]
Solvent	H ₂ O	MeOH + H ₂ O (1:1)	H ₂ O	MeOH + H ₂ O (1:1)	H ₂ O	MeOH + H ₂ O (1:1)	MeOH + H ₂ O (1:1)
Gel or not	Not gel	Not gel	gel	gel	gel	gel	gel
Peaks found	<i>a</i> [#]	0.58 ± 0.02	0.54 ± 0.01	0.55 ± 0.01	0.52 ± 0.01	0.52 ± 0.01	0.52 ± 0.01
(nm)	<i>b</i> [#]		1.17 ± 0.02	1.17 ± 0.02	1.26 ± 0.03	1.20 ± 0.02	1.15 ± 0.10
Others	1.47 ± 0.07	n/r*	2.45 ± 0.15	2.45 ± 0.12	2.45 ± 0.13	2.45 ± 0.15	2.89 ± 0.20

Note: #see text for definition of the dimensions *a* and *b*. *n/r = not resolved from

beamstop.

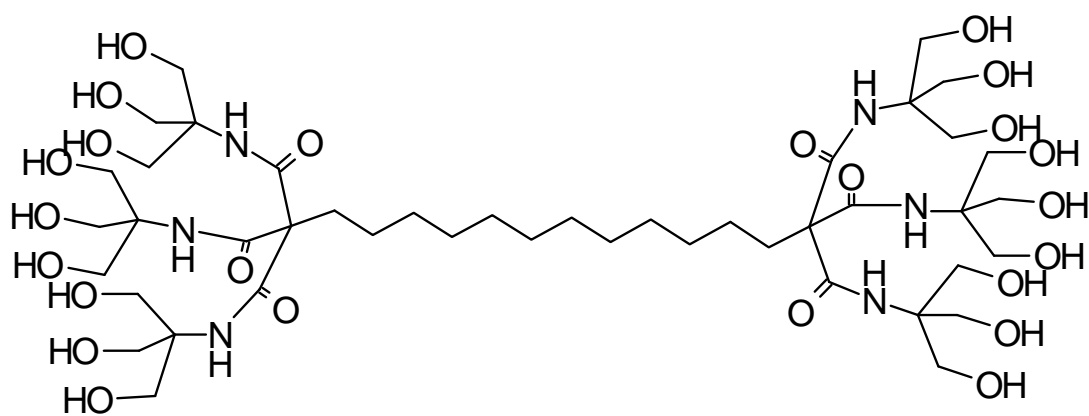


Figure 1. Structure of [9]-12-[9] arborol

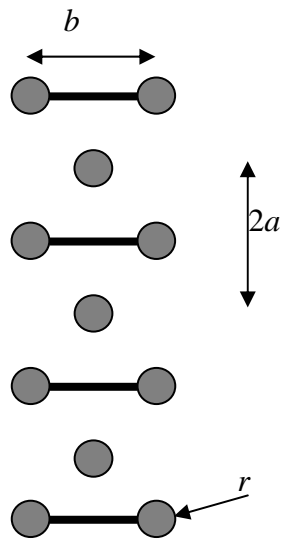


Figure 2. Model for single arborol fibers¹¹

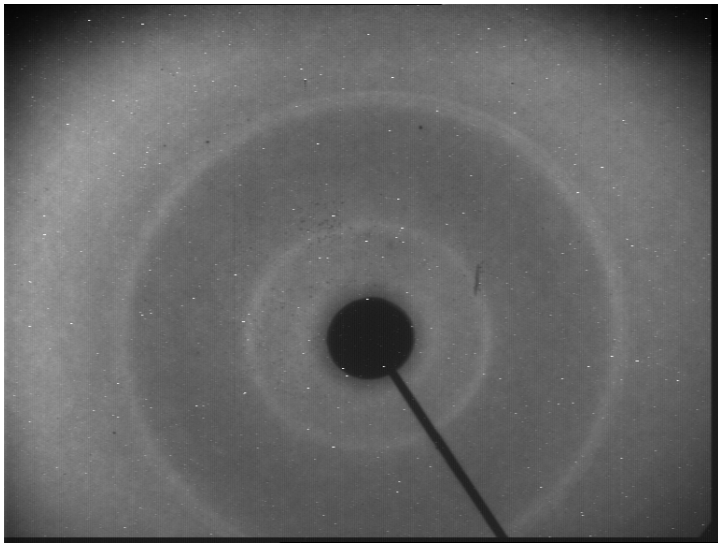


Figure 3. WAXS pattern for [6]-10-[6] in water.

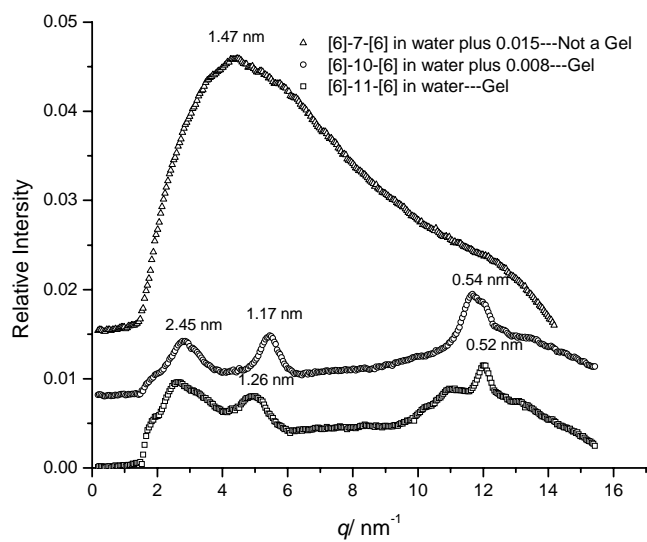


Figure 4. WAXS for [6]-*n*-[6] Arborols with Different Spacer Lengths in Water. Curves are offset vertically for clarity.

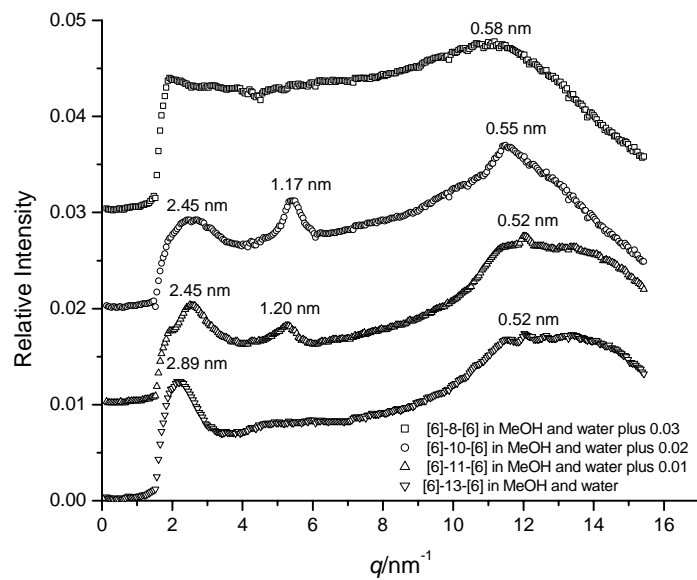


Figure 5. WAXS for [6]-*n*-[6] Arborols with Different Spacer Lengths in MeOH and Water. Curves are offset vertically for clarity.

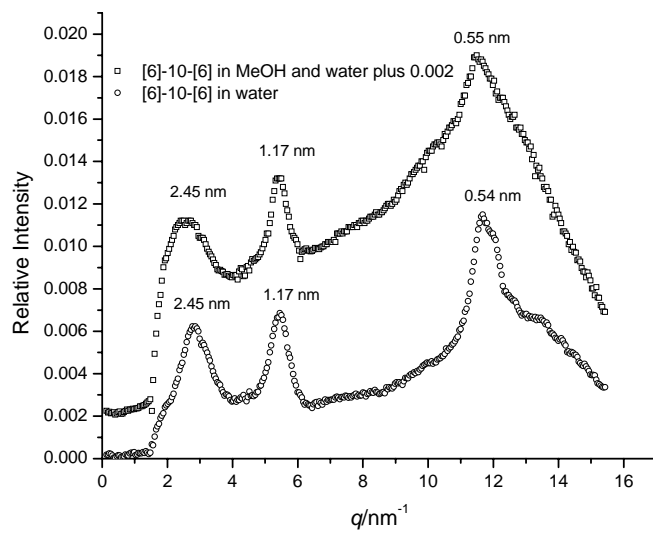


Figure 6. The Effect of Solvents on [6]-10-[6]. Curves are offset vertically for clarity.

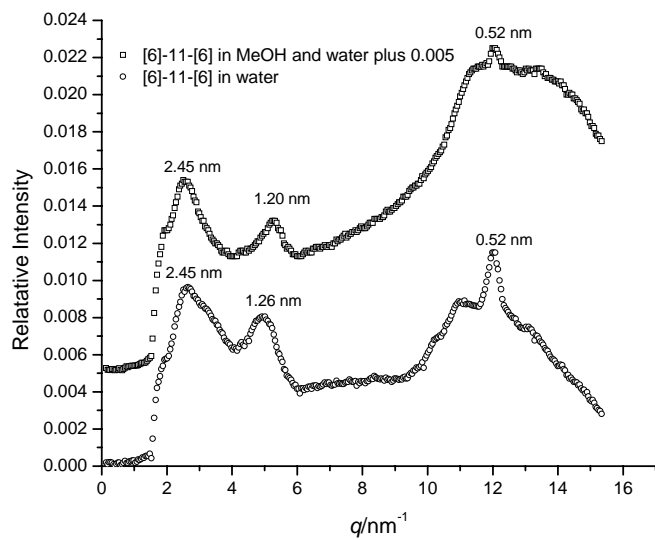


Figure 7. The Effects of Solvents on [6]-11-[6]. Curves are offset vertically for clarity.

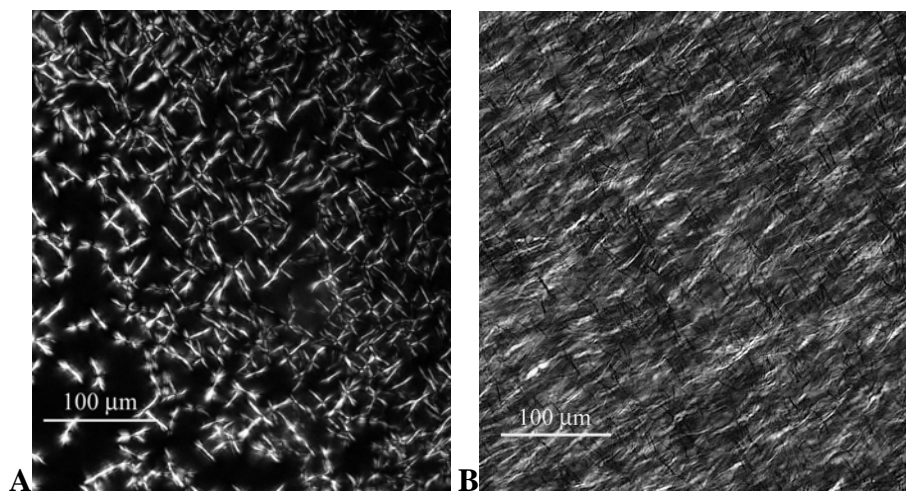


Figure 8. A 3 wt% [9]-12-[9] arborol gel, as viewed between crossed polar in an optical microscope. A: Unevenly distributed part of sample introduced by centrifuging; B: Evenly distributed part; C: View without polarizer.

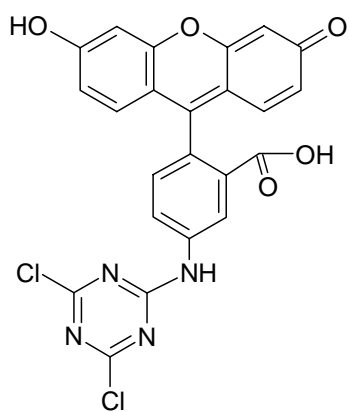


Figure 9. The Structure of 5-DTAF

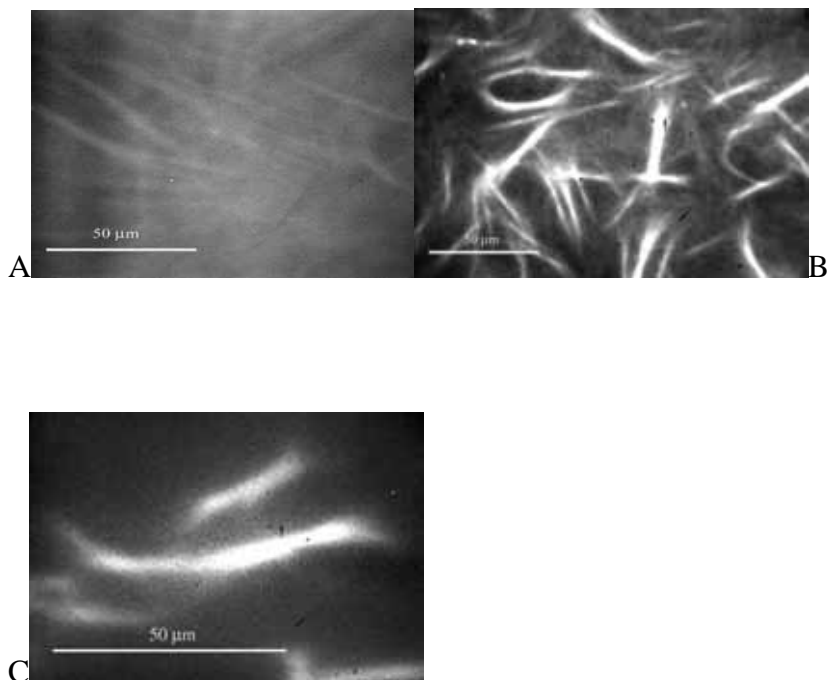


Figure 10. Fluorescence Microscopy of [9]-12-[9]. A. Confocal image taken from wet gel. B. Taken after the gel was dried. C. One specific spot in the dried gel.

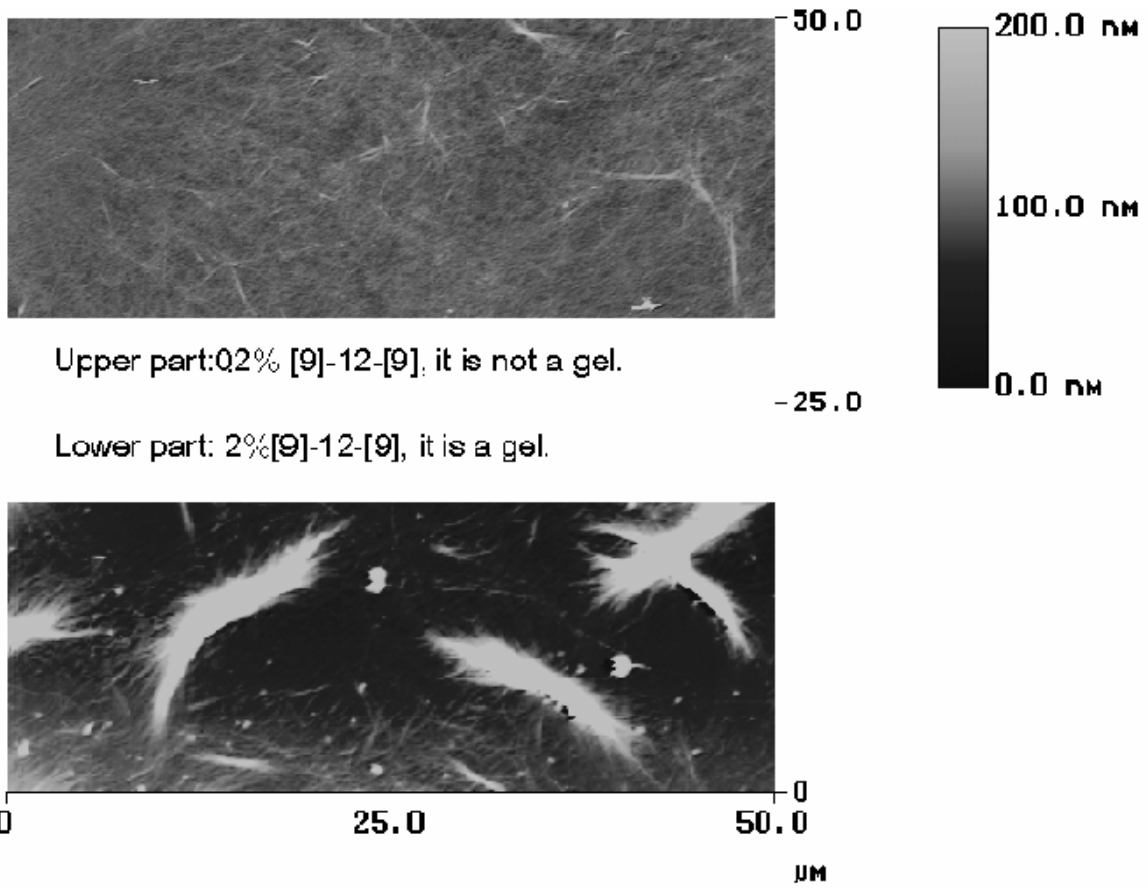


Figure 11. AFM image for 0.2% and 2% [9]-12-[9] in contact mode.